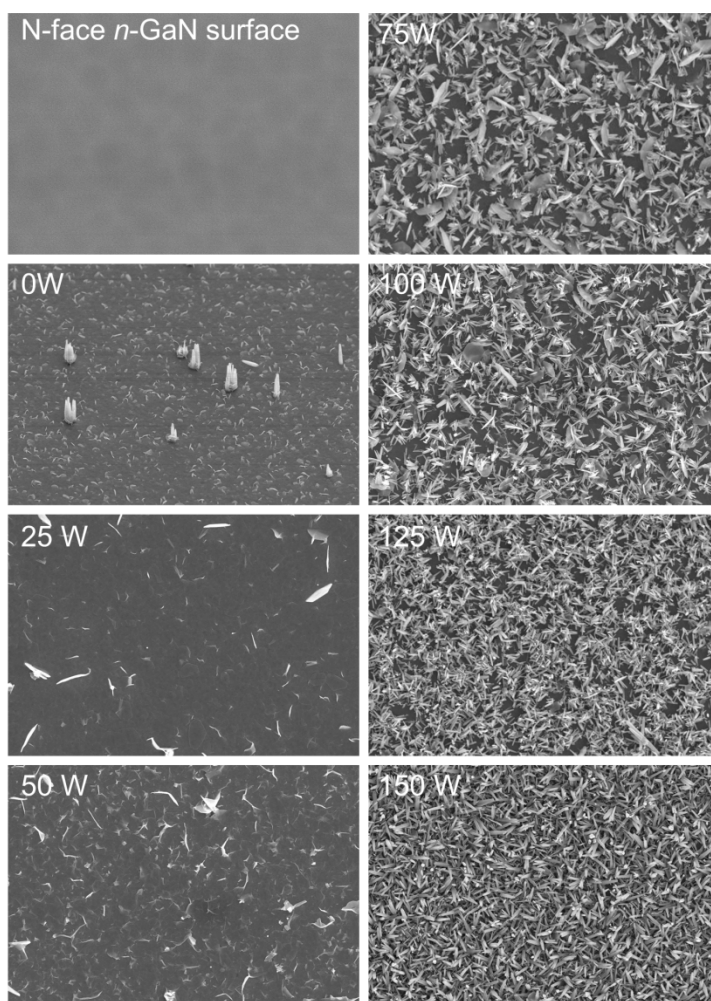


Electronic Supplementary Information

**Enhanced optical output power of InGaN/GaN vertical light-emitting diodes by ZnO nanorods on the plasma-treated N-face GaN**

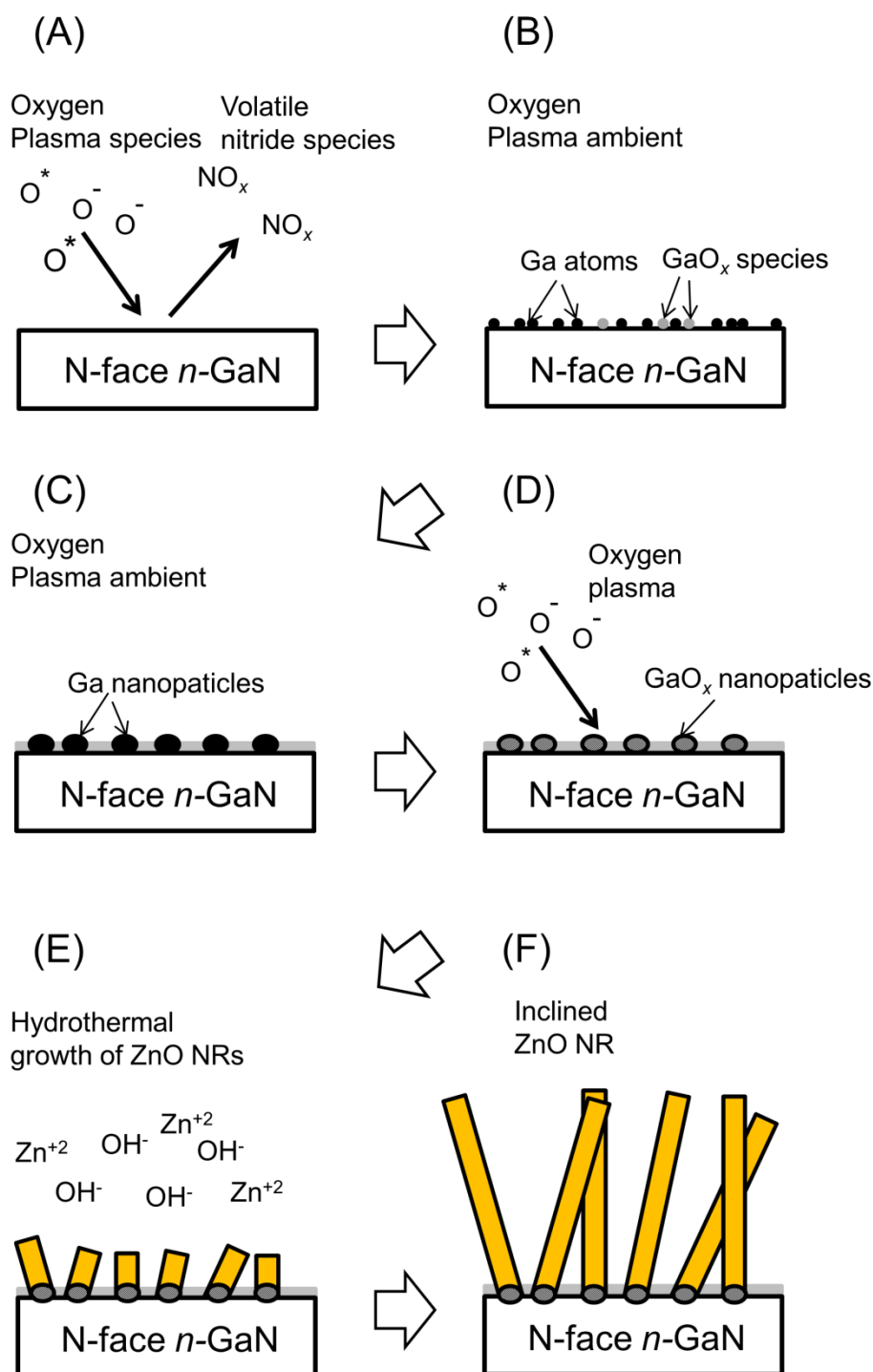
Young-Chul Leem,<sup>a</sup> Na-Yeong Kim,<sup>b</sup> Wantae Lim,<sup>c</sup> Sung-Tae Kim,<sup>c</sup> and Seong-Ju Park<sup>\*a,b</sup>



**Fig. S1.** SEM images of ZnO NRs on the N-face *n*-GaN surface as a function of radio frequency (RF) power during the oxygen plasma pretreatment. The density of ZnO NRs is increased with increasing the RF power.

Fig. S1 shows SEM images of ZnO NRs without and with oxygen plasma pretreatment using RF power in a range of 25 ~ 150 W on the N-face *n*-GaN layer, respectively. As shown in Fig. S1, the density of ZnO NRs on the N-face layer without oxygen plasma pretreatment is  $3.7 \times 10^6 \text{ cm}^{-2}$ , and the ZnO NRs are vertically oriented and well aligned along the  $[000\bar{1}]$  direction. However, the density of the ZnO NRs is increased with increasing the RF power of oxygen plasma pretreatment and the ZnO NRs are inclined at arbitrary angles. The density of

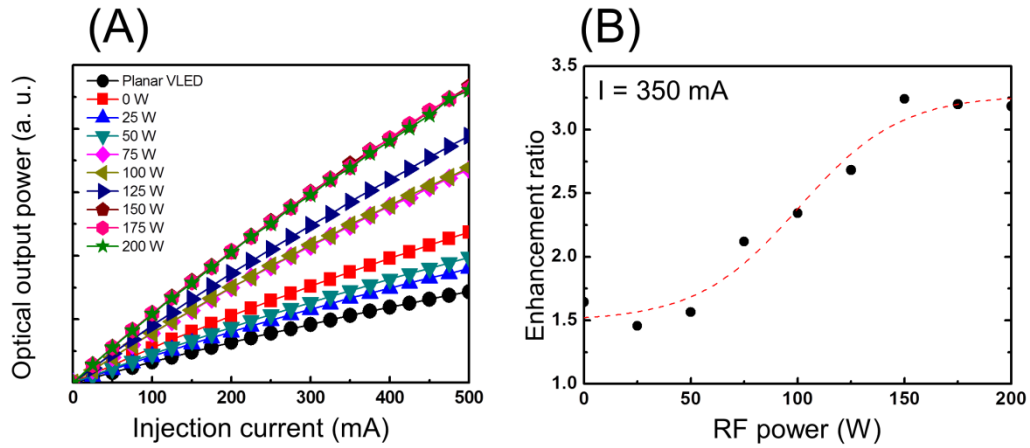
inclined ZnO NRs is drastically increased up to  $1.4 \times 10^9 \text{ cm}^{-2}$  following oxygen plasma pretreatment with 150 W of RF power.



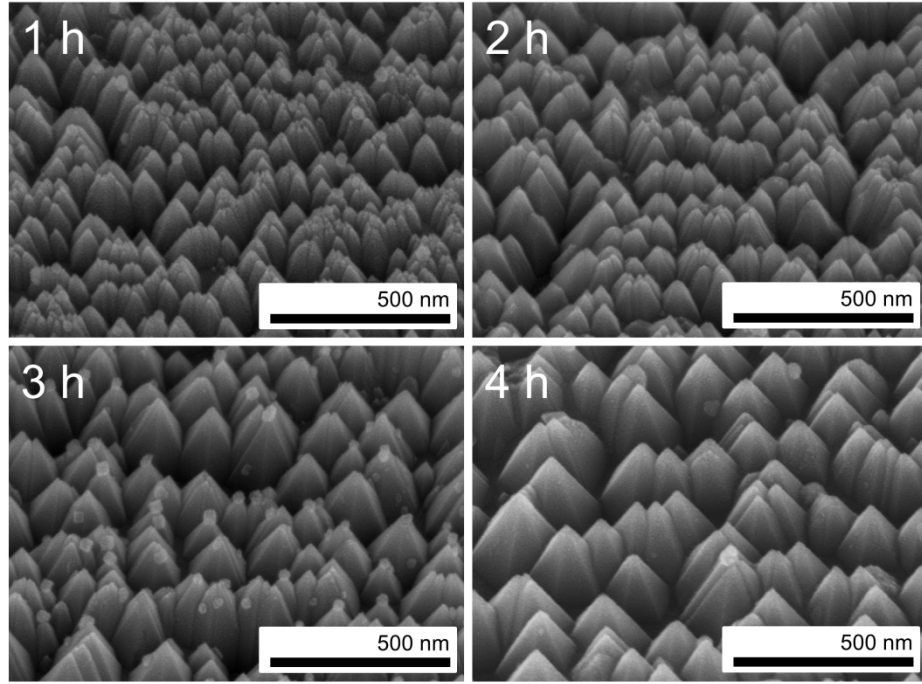
**Fig. S2.** Schematic illustration for a possible reaction processes on the N-face *n*-GaN surface during the oxygen plasma pretreatment and hydrothermal growth of dense and inclined ZnO NRs in the aqueous solution.

Fig. S2 schematically shows a possible reaction processes on the N-face *n*-GaN surface during the oxygen plasma pretreatment and hydrothermal growth of dense and inclined ZnO NRs. Highly active oxygen plasma species, such as oxygen radicals, react with the N-face surface, forming the volatile NO<sub>x</sub> species on the surface (Figure S2A). Then Ga atoms with dangling bonds owing to the N deficiency can be released from the surface of GaN epilayer by oxygen plasma bombardment and diffuse on the surface. The diffusing Ga atoms and nitrogen-poor Ga atoms attached to N-face surface can be further produced through the rearrangement of Ga atoms or formation of new bonds with O atoms of reactive oxygen plasma species (Figure S2B). And then, these Ga atoms reconstruct to Ga nanoparticles and the subsequently formed Ga nanoparticles loose the crystallinity at a low temperature of oxygen plasma pretreatment on the N-face GaN surface (Figure S2C). After the construction of Ga nanoparticles on the surface, the oxygen plasma species react with the Ga nanoparticles and convert them into GaO<sub>x</sub> (Figure S2D). Subsequently, the N-face *n*-GaN substrate with oxygen plasma pretreatment is dipped in an aqueous solution for the hydrothermal growth of ZnO NRs (Figure S2E). The solution used for the growth of ZnO NRs were zinc nitrate hexahydrate ((Zn(NO<sub>3</sub>)<sub>2</sub>·6H<sub>2</sub>O) as Zn sources and hexamethylenetetramine (HMTA, C<sub>6</sub>H<sub>12</sub>N<sub>4</sub>). The density of ZnO NRs is drastically increased after oxygen plasma pretreatment because the GaO<sub>x</sub> nanoparticles contribute greatly to the growth of the dense ZnO NRs on the N-face *n*-GaN surface as evidenced by the similar densities of ZnO NRs and GaO<sub>x</sub> nanoparticles on the surface after oxygen plasma treatment (Fig. 1C). The large increase in density of ZnO NRs indicates that the bound oxygen on the GaO<sub>x</sub> nanoparticles interrupts the diffusion of Zn atoms and reacts to form ZnO. Furthermore, vertical alignment of ZnO NRs on the N-face *n*-GaN surface is not plausible after oxygen plasma pretreatment because the ZnO nuclei can grow on the GaO<sub>x</sub> nanoparticles in any direction (Figure S2F). Therefore, ZnO NRs formed on the N-face *n*-GaN surface after oxygen plasma pretreatment are inclined

at arbitrary angles, whereas those without oxygen plasma pretreatment are vertically well aligned, as depicted in Fig. 1b and 1c.



**Fig. S3.** Light output power and enhancement ratio for ZnO NR VLEDs with different RF power during the oxygen plasma pretreatment compared to that of planar VLEDs. (A) Optical output power of VLEDs with wet-etched surface as a function of injection current from 0 to 500 mA. (B) Enhancement ratio of optical output power for ZnO NR VLEDs at an injection current of 350 mA as a function of RF power compared to planar VLED. These results indicate that the optimum RF power for growth of dense ZnO NRs on the N-face GaN surface is 150 W.



**Fig. S4.** SEM images of the N-face *n*-GaN layers with various etching time of 1, 2, 3, and 4 h in 2 M KOH solution. The density of hexagonal pyramid structures formed by the wet etching is decreased and the size of these structures is increased with increasing the etching time.

Fig. S4 shows SEM images of hexagonal pyramid structures formed on the N-face *n*-GaN surface by chemical wet etching process with different etching times from 1 to 4 h. To fabricate the surface textures, the samples were dipped into a 2 M potassium hydroxide (KOH) solution at room temperature. KOH can selectively etch GaN and produce hexagonal pyramid structures bound by the stable  $\{10\bar{1}1\}$  planes owing to the characteristic crystallographic etching of N-polarity *n*-GaN surfaces.<sup>1</sup> As shown in Fig. S4, the density of pyramid structures is decreased from  $1.6 \times 10^{10}$  (for 1 h) to  $6.2 \times 10^9$  cm<sup>-2</sup> (for 4 h) and this indicates that the density of etched cones decreases as the etch proceeds with time. However, the base of pyramid structures is increased from  $\sim 90$  (for 1 h) to  $\sim 200$  nm (for 4 h) with increasing the etching time due to coalescence of the pyramids.

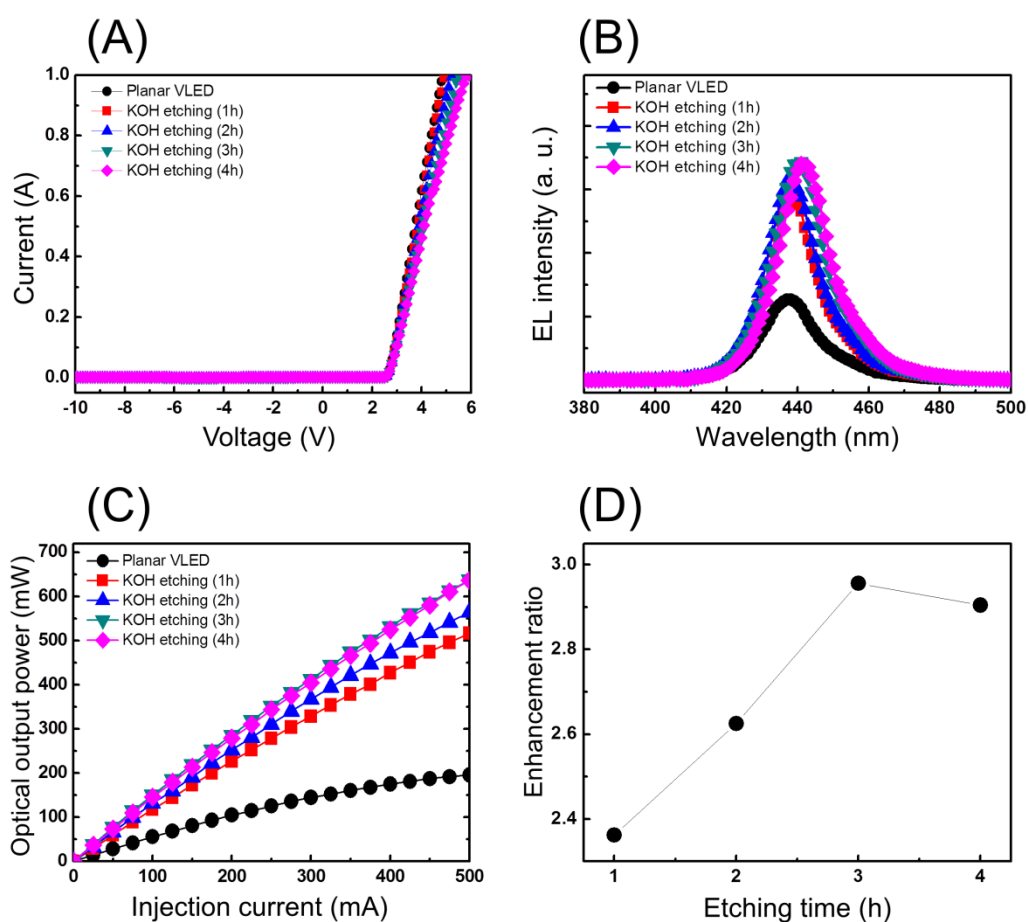


**Fig. S5.** Electrical and optical characteristics of VLEDs with wet-etched surface formed by KOH solution with various etching times and their comparison with those of planar VLEDs. (A) I–V characteristics of VLEDs with different etching times. (B) Room temperature EL spectra of VLEDs at an injection current of 350 mA. (C) Optical output power of VLEDs with wet-etched surface as a function of injection current. (D) Enhancement ratio of optical output power for VLEDs with wet-etched surface at 350 mA as a function of etching time compared to planar VLED.

The current–voltage (I–V) characteristics of the planar VLEDs and VLEDs with wet-etched surface with different etching times are shown in Fig. S5A. These results show that the forward voltages and series resistances are gradually increased from 3.39 to 3.7V and from 2.0 to 3.8  $\Omega$ , respectively, with increasing the etching time. The electrical deterioration of



VLEDs with etching time can be attributed to the additional defect states at the threading dislocations in the GaN layer and the reduced thickness of *n*-GaN layer acting as current channel.<sup>2</sup> Fig. S5B shows the electroluminescence (EL) spectra of the VLEDs with wet-etched surface measured at an injection current of 350 mA. As shown in Fig. S5B, the EL intensities of the VLEDs increase with increasing the etching time up to 3 h and the EL intensity is slightly decreased at the etching time of 4 h. Fig. S5C shows the light output power–current characteristics of VLEDs with wet-etched surface. The light output power of the VLEDs with different etching times of 1, 2, 3, and 4 h is enhanced by 2.36, 2.62, 2.96, and 2.90 times at 350 mA, respectively, compared to the planar VLEDs as shown in Fig. S5D. To compare the electrical and optical properties of these VLEDs with ZnO NR VLEDs, VLEDs with an etching time of 3 h were selected (Fig. 3).

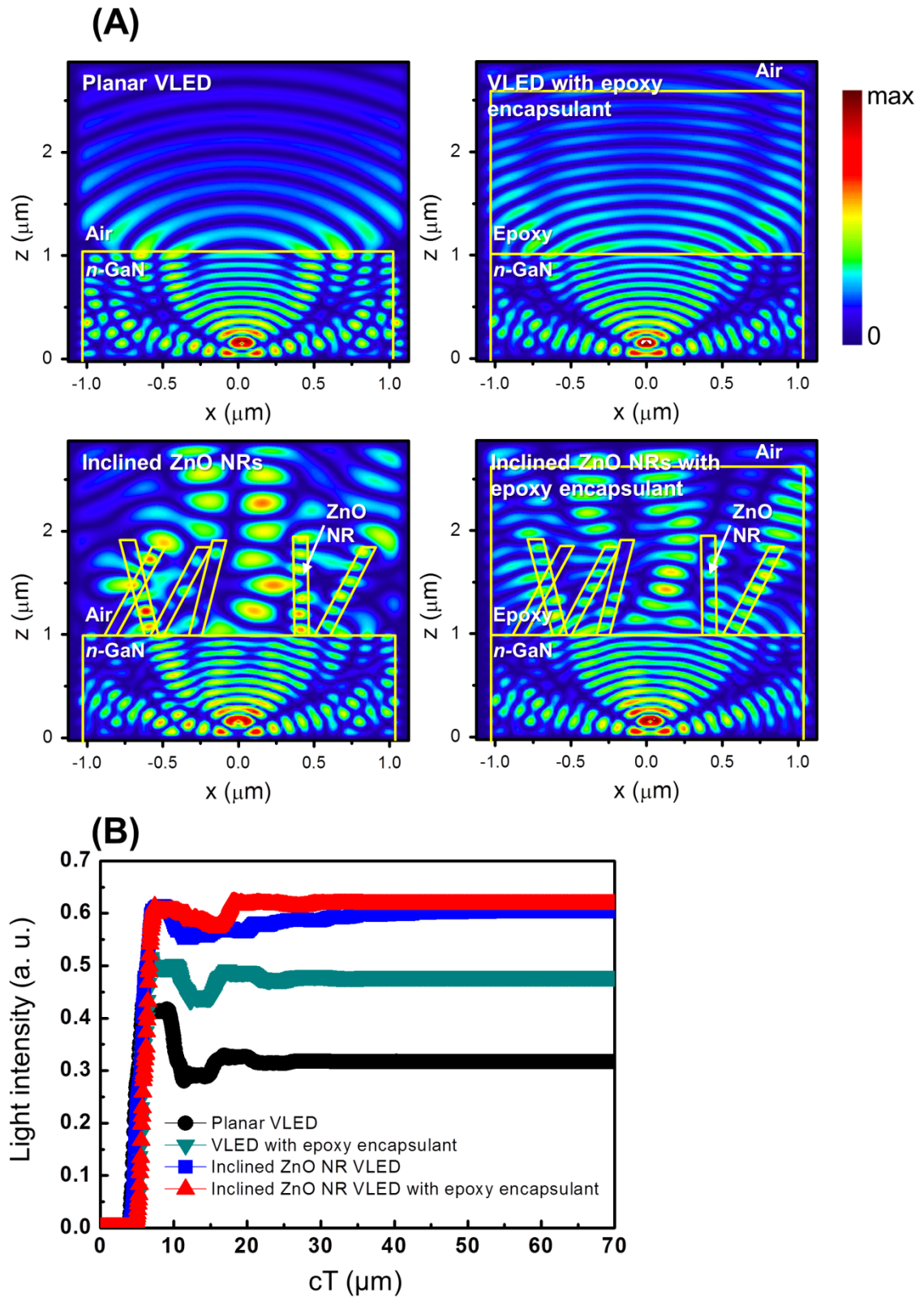


**Fig. S6.** Simulated light output power of planer VLED, VLED with epoxy encapsulant, and the inclined ZnO NRs VLED with and without epoxy encapsulant. (A) Simulated transverse

electric field intensity in VLED with different surface configurations. (B) Optical output power as a function of simulation time for VLED.

As mentioned above, VLEDs with dense and inclined ZnO NRs can greatly enhance the light extraction efficiency. However, ZnO NRs should be protected from moisture and physical damage by using epoxy encapsulant in LED package to use the ZnO NRs structures in practical VLED applications. To quantitatively demonstrate the effect of epoxy encapsulant on LEE of ZnO NR VLEDs, we carried out the finite difference time domain (FDTD) simulation. The diameter and height of ZnO NRs on the GaN layer are 165 and 910 nm, respectively, as determined from the SEM images presented in Fig. 1c. A monochromatic light source with an emission wavelength of 438 nm, matching with the emission peak in the EL spectra at an injection current of 350 mA, is located in the GaN layer. In addition, we assume that epoxy encapsulant covers the topside of the GaN layer with or without the inclined ZnO NRs and the thickness of epoxy encapsulant is varied to optimize the optical output power of ZnO NR VLED with epoxy encapsulant. The simulated intensity of transverse electric field for planar VLED, VLED with 1.57  $\mu\text{m}$ -thick epoxy encapsulant, and the inclined ZnO NRs VLED with and without epoxy encapsulant (1.64  $\mu\text{m}$ ) is depicted in Fig. S6A. Fig. S6B shows the calculated optical output of these VLEDs. The optical output power of the inclined ZnO NR VLEDs containing epoxy encapsulant with an optimized thickness of 1.64  $\mu\text{m}$  is higher by a factor of 3.76 compared to the planar VLEDs. The slight enhancement in optical output power compared to that of the inclined ZnO NR VLEDs without epoxy encapsulant ( $\sim 3.6$  times) indicates that the epoxy encapsulant can be used to protect the ZnO NRs from the moisture and physical damage without losing the LEE in the commercialized LED package.

## References

1. Y. Gao, T. Fujii, R. Sharma, K. Fujito, S. P. Denbaars, S. Nakamura and E. L. Hu, *Jpn. J. Appl. Phys.*, 2004, **43**, L637.
2. Y. Gao, M. D. Craven, J. S. Speck, S. P. Den Baars and E. L. Hu, *Appl. Phys. Lett.*, 2004, **84**, 3322.